https://doi.org/10.1016/j.buildenv.2016.12.032
This is the Pre-Published Version.

CFD simulation of flow in a long street canyon under a perpendicular wind direction: evaluation of three computational settings

Z.T. Ai
Department of Building Services Engineering, The Hong Kong Polytechnic University, Hong Kong
E-Mail: zhengtao.ai@connect.polyu.hk; zheai@byg.dtu.dk

C.M. Mak (Corresponding author)
Department of Building Services Engineering, The Hong Kong Polytechnic University, Hong Kong
Tel.: +852 2766 5856; Fax: +852 2765 7198
E-Mail: cheuk-ming.mak@polyu.edu.hk

Abstract: A street canyon is an important platform for the understanding of local atmospheric flow and other related processes in the built environment. Many previous studies focused on long street canyons under a perpendicular wind direction, as they represent the worst street canyon microclimate, such as stagnation of wind and accumulation of pollutants. While CFD simulations were widely applied to investigate atmospheric processes in street canyons, appropriate computational settings are important factors influencing the predictive reliability. A non-exhaustive literature review of CFD studies on atmospheric processes in long street canyons indicates an arbitrary selection of three important computational settings, namely computational domain configuration, domain dimensions and inflow boundary conditions. Based on previous water tunnel experimental data for street canyons with aspect ratio equal to 0.5, 1.0 and 2.0, this study evaluates the influence of the three computational settings on CFD prediction of isothermal flow field inside the street canyons. Flow field inside an urban street canyon cannot be reasonably predicted using an isolated street canyon included in a conventional computational domain, which, however, can be well predicted using a T-shape computational domain where a street canyon is connected to a free flow layer above the canyon. A T-shape domain with the upstream length, downstream length and height above a street canyon all equal to the height of the street canyon is appropriate when considering both computational cost and predictive accuracy. It is reasonable to use uniform inflow boundary conditions to represent the free layer above street canyons.

Keywords: Street canyon; Flow; CFD; Computational domain; Boundary conditions

1. Introduction

As a basic unit of urban areas, a street canyon is an important platform for the understanding of the local atmospheric flow and other related processes in the built environment [1]. Microclimate in urban street canyons, including particularly flow, temperature, pollutants and noise, not only determines the outdoor environmental quality, but also has a close association with the indoor environmental quality in their nearby buildings [2]. A significant amount of work investigating atmospheric processes in street canyons using a wide range of methods has been published in the past decades.

On-site measurement is a straightforward research method to reveal the real-world street canyon microclimate including the lowered wind speed [3-9] and the elevated pollutant concentration [10-13]. However, this method is influenced by many factors including especially the constantly varying meteorological conditions. In comparison, reduced-scale wind/water tunnel experiments can take a good control over the boundary conditions, which reveal detailed wind flow structures and pollutant dispersion mechanisms in street canyons [14-22]. However, reduced-scale experiments are sometimes limited by similarity requirements [23-25]. In addition, both on-site measurements and wind/water tunnel experiments are only performed at a limited number of selected points, which do not provide a whole image of the flow and concentration fields. As an alternative method, computational fluid dynamics (CFD) simulation provides whole-field data at no expense of similarity requirements.

© 2016. This manuscript version is made available under the CC-BY-NC-ND 4.0 license https://creativecommons.org/licenses/by-nc-nd/4.0/.

Although validations of CFD models against physical experiments are required, CFD simulation is applied intensively on studies regarding street canyon related atmospheric processes [20, 26-32].

It is well known that the accuracy and reliability of CFD simulations are strongly influenced by the computational settings, including the physical geometry, computational domain dimensions, grid quality, boundary conditions, solution methods and convergence criteria. There are some best practice guidelines [33-36] providing general guidelines for CFD simulation of urban aerodynamics, which covers almost all aspects of the above mentioned computational settings. In addition, some literature provides very detailed guidelines on specific aspects or research problems, such as the achievement of homogeneous atmospheric boundary layer along computational domain [37-42] and natural ventilation [43-44]. However, to the best knowledge of the authors, there are no specific guidelines for CFD simulation of atmospheric processes in street canyons, which may have some special aspects being different from the common knowledge of CFD simulation of urban aerodynamics.

A non-exhaustive literature review (see Figure 1 and Table 1) of wind tunnel and CFD studies of atmospheric processes in street canyons in recent years shows that six different configurations of experimental/computational domain were commonly used. Note that the Domains C and D are similar with those used for studies of general atmospheric processes around building(s) protruding over the ground. In Domains A, B, E and F, the length of the street canyons is the same as or very close to the width of the domain. The four domains are usually used to simulate the long street canyons, where the two dimensionality appears on the vertical centerplane of the street canyon(s). Among the six domain configurations, Domains B and C are most widely used in wind tunnel experiments, while Domains E and F are most widely adopted in CFD simulations. Although the selection of street canyon(s) and domain configurations in both wind tunnel experiments and CFD simulations is normally compromised by the available resources (e.g., dimensions of wind tunnel or computational power), it is critically important that a selection can achieve the research objectives. For the six different domain configurations, a comparison of the flow patterns inside the target street canyon is urgently needed to recommend the appropriate configurations that can represent as close as possible the real-world situations.

The literature review also shows that the selection of domain dimensions and the inflow boundary conditions seems to be arbitrary. Taking the literature using Domain E as an example (see Table 2), the domain height above a street canyon varies from 1.0 to 8.0 times of the height of the street canyon and the inflow boundary conditions include uniform, power-law and logarithmic-law velocity profiles. The influence of the domain dimensions and the inflow boundary conditions on the flow patterns inside a street canyon still awaits evaluations.

It is evident that flow problems in a single street canyon are receiving wide attentions because of its important role in understanding basic flow structures and pollutant dispersion mechanisms in urban areas. Owing to many advantages, CFD simulation has become the most widely used research method to study atmospheric processes in a street canyon. However, the literature review of previous CFD studies indicates arbitrary selections of computational domain, domain dimensions and inflow boundary conditions. These arbitrary selections should be partially attributed to the fact that they are not included in the general BPG for CFD simulation of urban aerodynamics. These computational settings have significant influences on the accuracy and reliability of the predicted flow field. Therefore, the objective of this study is to evaluate the three computational settings and then suggest appropriate selections from the viewpoints of both predictive accuracy and computational costs. Atmospheric processes in a street canyon include wind-induced flow, buoyancy-induced flow, pollutants dispersion, traffic-induced turbulence and so on. This study focuses on only the isothermal flow, given that it is the basic element for understanding and predicting other processes. The water tunnel experiments [16] based on street canyons with AR (aspect ratio) equal to 0.5, 1.0 and 2.0 are used to validate CFD model. The validated CFD model is then used to evaluate the three computational settings. First, the six domain configurations (see Figure 1) are examined and the flow field inside the street canyons are compared. Second, the influence of the dimensions of the domain

suggested in the first step is then examined. Third, based on the domain configuration and dimensions resulted from the previous two steps, two types of inflow boundary conditions, namely the uniform and logarithmic-law inflow boundary conditions, are compared. This study is conducted based on the most widely used RANS turbulence model, namely renormalization group (RNG) $k-\varepsilon$ model. The findings of this study are intended to provide information and suggestions for future CFD simulations of flow and related processes in urban street canyons.

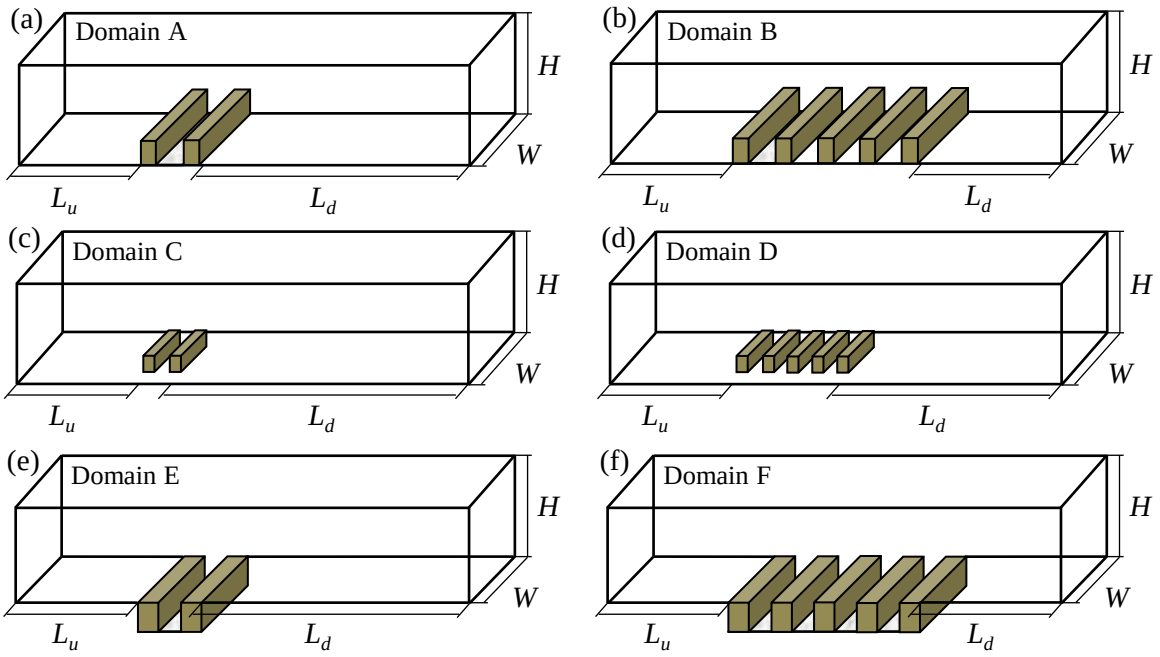

Figure 1 Schematic view of computational domains used in previous wind tunnel and CFD studies; in this figure, it should be noted that first (b), (d) and (f) represent those studies using more than 2 buildings in their street canyon configurations and second (a), (b), (e) and (f) may also represent those performing only two-dimensional CFD simulations. The literature using the above street canyon configurations and computational domains is listed in Table 1.

Table 1 A summary of the literature using the street canyon configurations and computational domains illustrated in Figure 1.

Domain configurations	Wind tunnel experiments		CFD simulations	
	Authors (year)	Ref.	Authors (year)	Ref.
Domain A	Baik et al. (2000)	[14]	So et al. (2005)	[45]
Domain B	Pavageau and Schatzmann (1999); Kastner-Klein and Plate (1999); Li et al. (2008a); Salizzoni et al. (2009); Kellnerova et al. (2012)	[15], [16], [17], [18], [46]	Nazridoust and Ahmadi (2006); Mirzaei and Haghighat (2011); Kikumoto and Ooka (2012)	[47], [48], [49]
Domain C	Kastner-Klein et al. (2001); Gromke et al. (2008); Buccolieri et al. (2009, 2011); Stabile et al. (2015)	[19], [20], [21], [50], [51]	Gromke et al. (2008); Solazzo et al. (2008); Salim et al. (2011); Moonen et al. (2013)	[20], [52], [53], [54]
Domain D	Kastner-Klein and Plate (1999)	[46]	Not found	
Domain E	Allegrini et al. (2013)	[22]	Kim and Baik (2001);	[26], [27], [28],

		Liu et al. (2004); Xie et al. (2006); Baik et al. (2007); Li et al. (2008); Kumar et al. (2009); Hu et al. (2009); Moonen et al. (2011); Zhang et al. (2011); Baik et al. (2012); Kwak et al. (2013); Allegrini et al. (2014); Madalozzo et al. (2014)	[29], [30], [31], [55], [56], [57], [58], [59], [60], [61]
Domain F	Not found in this small-scale review	Assimakopoulos et al. (2003); Xie et al. (2007); Cheng et al. (2009); Cheng and Liu (2011); Liu et al. (2011); Takano and Moonen (2013); Hang et al. (2016)	[32], [62], [63], [64], [65], [66], [67]

Table 2 A summary of the domain height, inflow velocity profile and turbulence model used in previous CFD simulations using the Domain E, where H_B represents the height of street canyon and RANS means Reynolds-averaged Navier-stokes.

References	Ref.	AR	Domain height above the street canyon	inflow velocity profile	Turbulence model
Kim and Baik (2001)	[26]	0.6-3.6	0.1-5.7 H_B	Power law	RANS-Standard $k-\varepsilon$
Liu et al. (2004)	[27]	0.5-2.0	1.0 H_B	Uniform	LES
Xie et al. (2006)	[28]	0.17-3.5	7.0 H_B	Uniform	RANS-Standard $k-\varepsilon$
Baik et al. (2007)	[55]	1.0	2.0 H_B	Logarithmic law	RANS-RNG $k-\varepsilon$
Li et al. (2008)	[56]	1.0-5.0	1.0 H_B	Uniform	LES
Kumar et al. (2009)	[57]	1.0	5.0 H_B	Uniform	RANS-Standard $k-\varepsilon$
Hu et al. (2009)	[58]	1.0	1.2 H_B	Uniform	LES
Moonen et al. (2011)	[29]	1.0	8.0 H_B	Logarithmic law	RANS-Realizable $k-\varepsilon$, LES
Zhang et al. (2011)	[59]	1.0	1.0 H_B	Uniform	LES
Baik et al. (2012)	[60]	1.0	2.0 H_B	Logarithmic law	RANS-RNG $k-\varepsilon$
Kwak et al. (2013)	[30]	1.0-2.0	2.0-2.5 H_B	Logarithmic law	RANS-RNG $k-\varepsilon$
Allegrini et al. (2014)	[31]	1.0	4.275 H_B	Fitted from wind tunnel experiments	RANS-Standard $k-\varepsilon$, Realizable $k-\varepsilon$
Madalozzo et al. (2014)	[61]	0.5-2.0	2.0-7.0 H_B	Power law	LES

2. CFD simulations: base case and model validation (AR=1.0)

2.1. Description of the water tunnel experiments

Li et al. [16] measured flow field inside a target street canyon in a water tunnel ($L_T \times W_T \times H_T$: 10 m × 0.3 m × 0.5 m). Street canyons were formed by eight identical building models ($L_B \times W_B \times H_B$: 0.3 m × 0.1 m × 0.1 m), which were placed perpendicularly to the prevailing flow direction in the working test section (see Figure 2). The height of the buildings was fixed at H_B = 0.1 m, while the width of the street canyons W_S was varied to form different aspect ratios (H_B/W_S), including 0.5, 1.0 and 2.0. Velocity components in the streamwise and vertical directions on the centerplane (y = 0) were measured using a two-colour laser Doppler anemometer (LDA). The depth of water in all experiments was 0.4 m. The Reynolds number based on the reference velocity (U_{ref}) in freestream at z = 0.3 m and the building height was around 12,000, meaning that U_{ref} is equal to 1.8 m/s. There were no roughness elements on the tunnel ground. The case with AR equal to 1.0 was investigated in this section, while the cases with ARs equal to 0.5 and 2.0 are investigated in Section 4. The flow speed was measured along three vertical lines and two horizontal lines on the vertical centerplane of the target street canyon (see Figure 2 (a)).

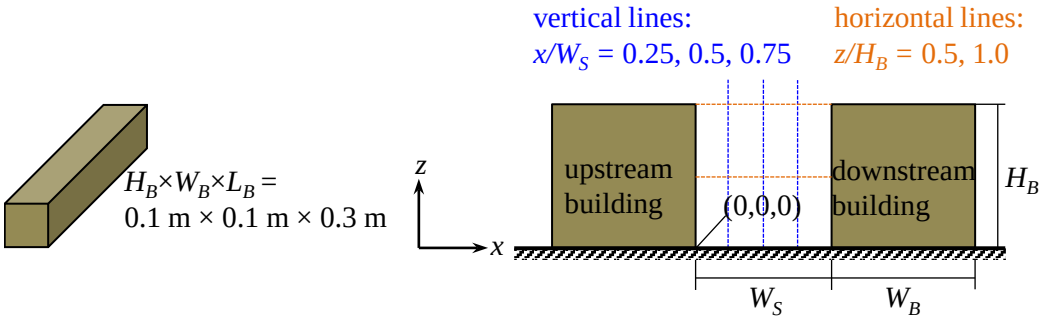

(a) building model and the vertical centerplane of the target street canyon model

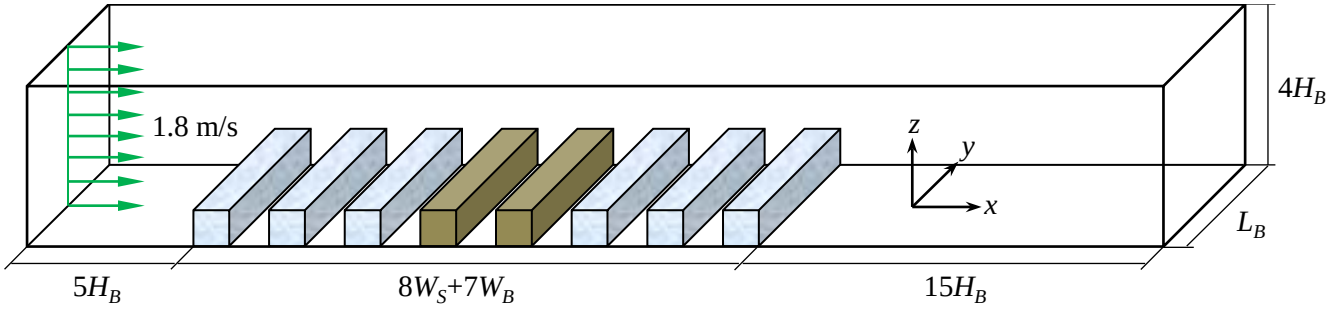

(b) computational domain

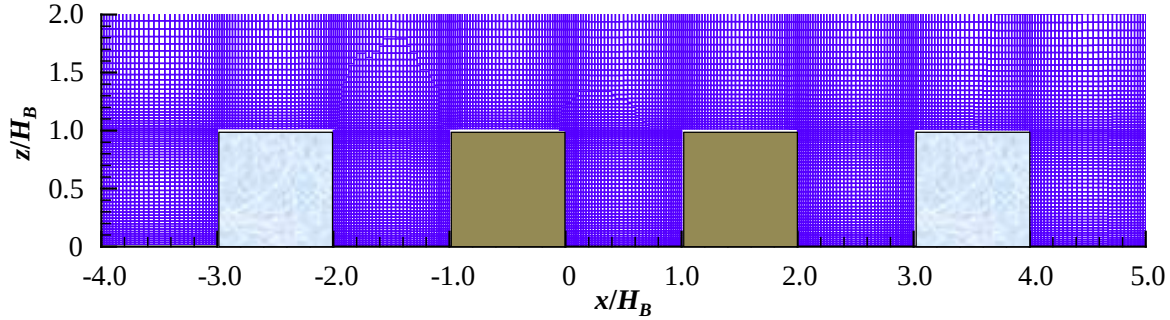

(c) mesh information on part of vertical centerplane

Figure 2 The street canyon model, computational domain and mesh information.

2.2 Computational settings and parameters

The building model and street canyon model used in CFD simulations are the same with those in the water tunnel experiments (see Figure 2 (a) and (b)). This configuration of computational domain represents the Domain B as shown in Figure 1. Selection of domain dimensions (see Figure 2 (b)) is based on the existing best practice guidelines for CFD simulation of urban aerodynamics [34-35], except that the height and lateral length of the domain follow those in water tunnel experiments. Particularly, the street model extends across the domain width in y direction, meaning that infinitely long street canyons are considered. Structured hexahedral cells are used to construct the whole computational domain (see Figure 2 (c)). This very fine grid, with 3,168,000 cells in total, is selected after a grid sensitivity test. The numbers of cells along building height, width and length in z, x, y and directions are 40, 40 and 80, respectively. The height of the first cells near the ground and walls is 1.665 mm, which yields the y^+ values at these first cells ranging between 0 and 15, with an average value equal to 5.3. Large y^+ values occur only at the top corners of the windward facades.

Same with that in the experiments, a uniform flow speed at 1.8 m/s is specified at the inlet of the computational domain. The experimenters do not provide the turbulence characteristics of the inflow. The turbulent length scale is determined first based on the hydraulic diameter of the wetted cross-section of the water tunnel (that is 0.35 m). A sensitivity test against the experimental data for velocity field is then conducted to determine the turbulent intensity (that is 5%). Pressure outlet with zero static pressure is defined at the domain outlet. At the lateral sides and the top of the domain, zero normal velocity and zero normal gradients of all variables are defined [42]. The domain ground and the building surfaces are defined as non-slip walls. Owing to two reasons, there is no roughness height being defined at the domain ground. The first reason is that there were no roughness elements on the ground of the water tunnel [16]. The second reason is that the multiple street canyons in the upstream and downstream of the target street canyon serve to create a roughness effect of an urban area.

Commercial CFD code ANSYS Fluent 13.0.0 [68] is used to conduct the numerical simulations. A steady-state two-equation RANS model, namely RNG $k-\varepsilon$ model [69], is employed to predict the flow and turbulence fields. RNG $k-\varepsilon$ model is selected due to its general good performance in predicting flow around buildings [60, 70-72]. Based on the very fine grid as shown in Figure 2 (c), the two-layer model [73] is used by RNG $k-\varepsilon$ model to treat the near-wall regions. SIMPLEC algorithm is used for coupling pressure and momentum equations. The second-order schemes are used to discrete the convection and diffusion terms. Convergence is achieved when all scaled residuals are less than 10^{-5} and the average flow speeds at several locations within the target street canyon are stable for over 50 iterations.

2.3 Comparison between CFD and experimental results

Figure 3 presents the velocity contour on the vertical centerplane of the street canyon model, from which two main observations can be made. First, owing to the flow impingement and separation at the windward facade of the first building model, the flow pattern in the first two street canyons are affected largely and thus different obviously from those in their downstream street canyons. The downstream wake effect of the last building model also presents some influences on the flow pattern in its upstream street canyons. This observation may suggest that it is not reasonable to use an isolated street canyon to investigate the general flow pattern inside a street canyon in an urban area. Second, the skimming flow above the street canyons, e.g. that above the building models 4-7, tends to be stable, which is an important sublayer of the atmospheric boundary layer in urban areas. This relatively stable atmospheric flow skimming over the building tops may be represented using flow profiles as similar with those above ground.

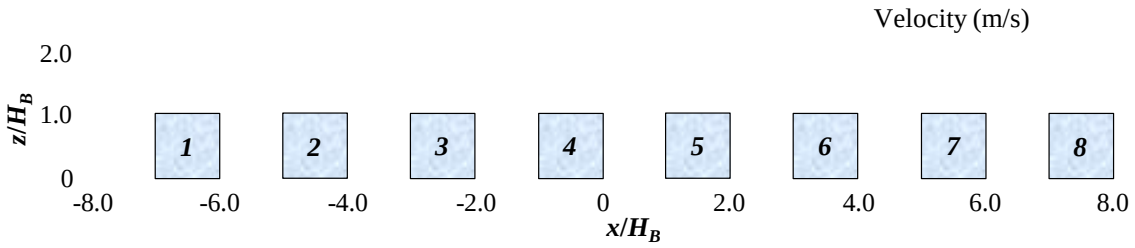

Figure 3 Predicted velocity contour on the vertical centerplane of the street canyon model.

Figure 4 presents the velocity vector on the vertical centerplane of the target street canyon, where the experimental results from another water tunnel experiment [14] are also presented for comparison. For the street canyon with an aspect ratio equal to 1.0, one vortex is formed. The location of the vortex center predicted by the CFD model is very close to that obtained in experiments. Figure 5 shows the velocity components in x and z directions along vertical and horizontal lines on the vertical centerplane of the targe street canyon. It can be seen that the CFD model predicts a very accurate flow field within the street canyon when compared to the experimental data, except for the vertical velocity component w along the center line x/W_S = 0.5 (see (iv) in Figure 5 (a)). On this center line, the w predicted by the RNG $k-\varepsilon$ model is close to zero, which should be attributed to that the time-averaged treatment of RNG theory tends to cancel out some of the fluctuating velocity pulses. In general, the RNG $k-\varepsilon$ model can accurately predict the flow field in the street canyon, which justifies the use of it in the rest of this paper.

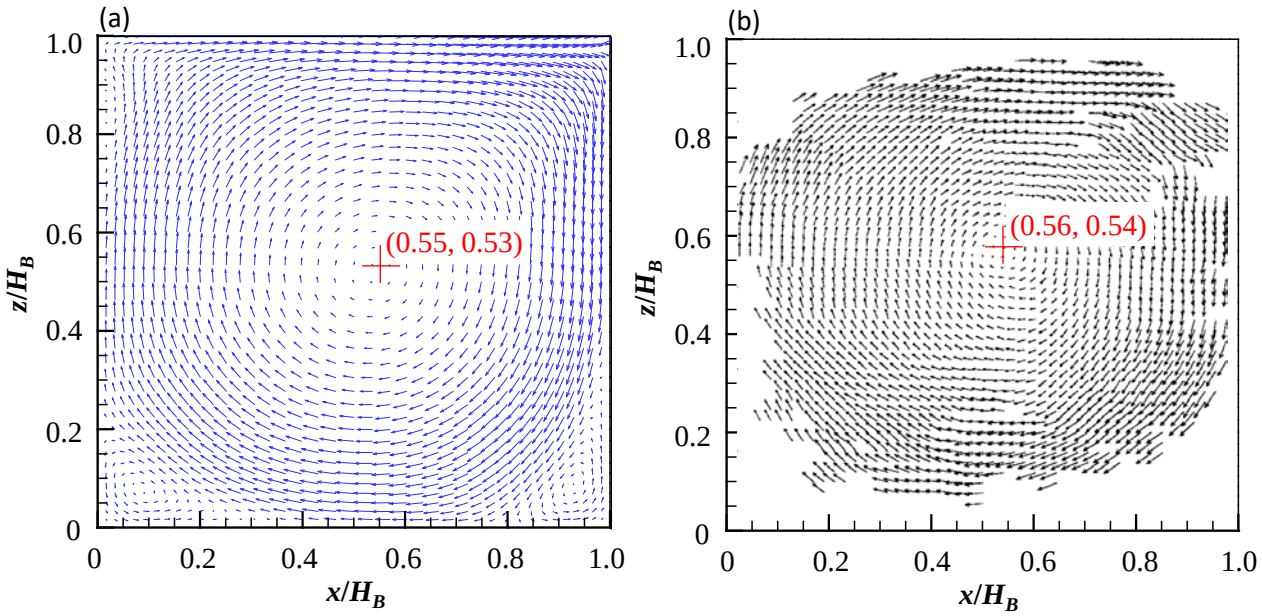

Figure 4 Velocity vector on the vertical centerplane of the target street canyon; the red symbol (+) marks the physical canter of the vortex and the numbers in the parentheses represent (x/H_B, z/H_B): (a) CFD results and (b) water tunnel results [14].

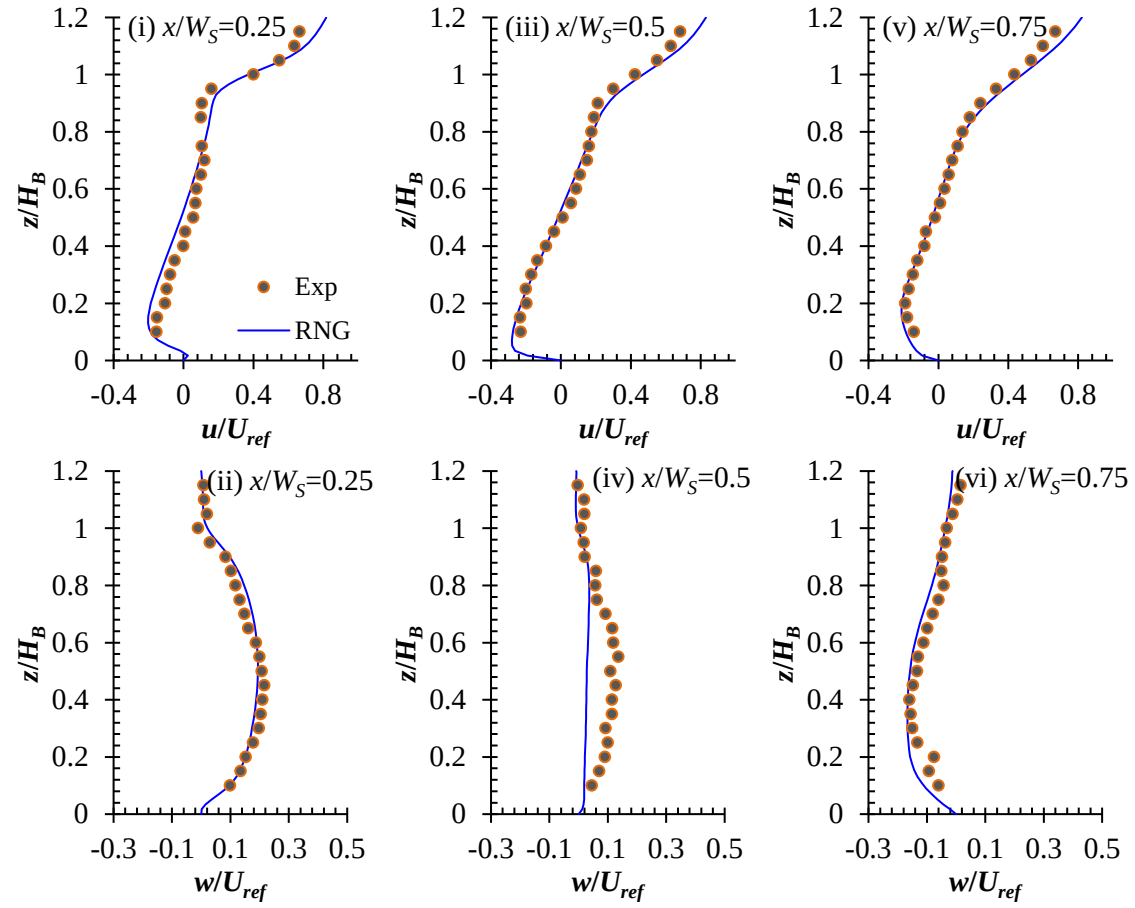

(a) vertical lines

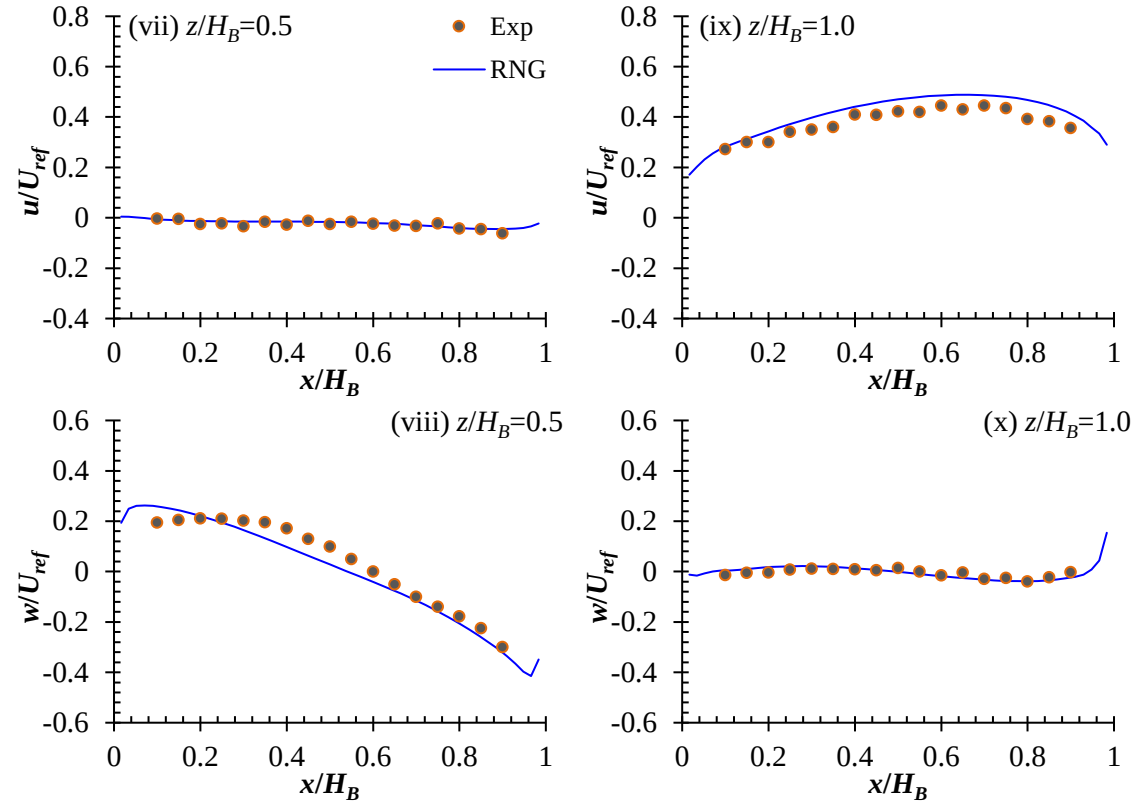

(b) horizontal lines

Figure 5 Velocity components in x and z directions along three vertical and two horizontal lines on the vertical centerplane of the target street canyon.

3. Evaluation of computational settings (AR=1.0)

This section evaluates the influence of computational domain configuration, domain dimensions and inflow boundary conditions on the prediction of flow field in a street canyon in an urban context (namely, not an isolated street canyon). It is intended to explore appropriate computational settings when considering both the predictive accuracy and the computational cost.

3.1 Evaluation of computational domain configuration

In addition to the Domain B (see Figure 1 and Figure 2), other three computational domains, namely Domain A, Domain E and Domain F (see Figure 1 and Figure 6), are adopted to predict the flow field inside a same street canyon and the results are compared. The Domain C and Domain D (see Figure 1) are theoretically excluded because they are first computationally more expensive than other domains and second influenced largely by the length of the street canyon. Note that the general computational settings are the same with those described in Section 2, except for the computational domain configuration.

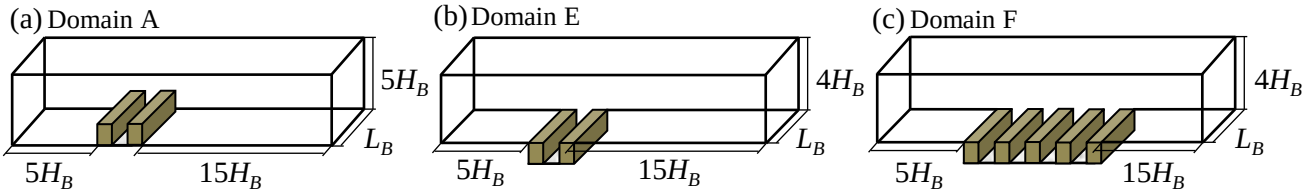

Figure 6 Schematic view of domain configurations used for evaluation; note that the number of buildings in Domain F is the same as that in Section 2.

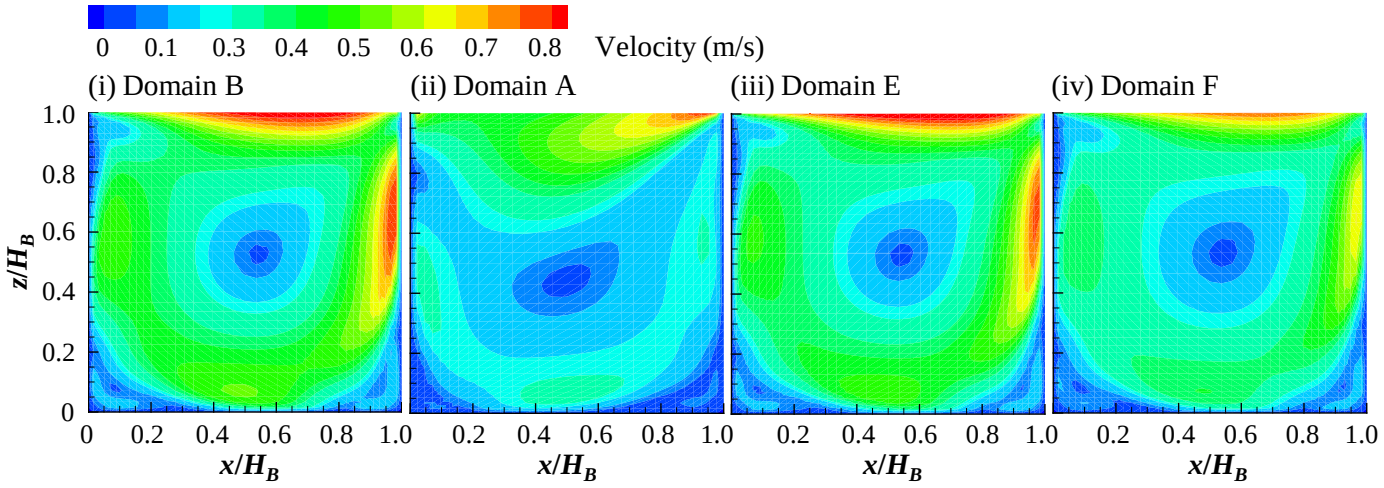

(a) velocity contour

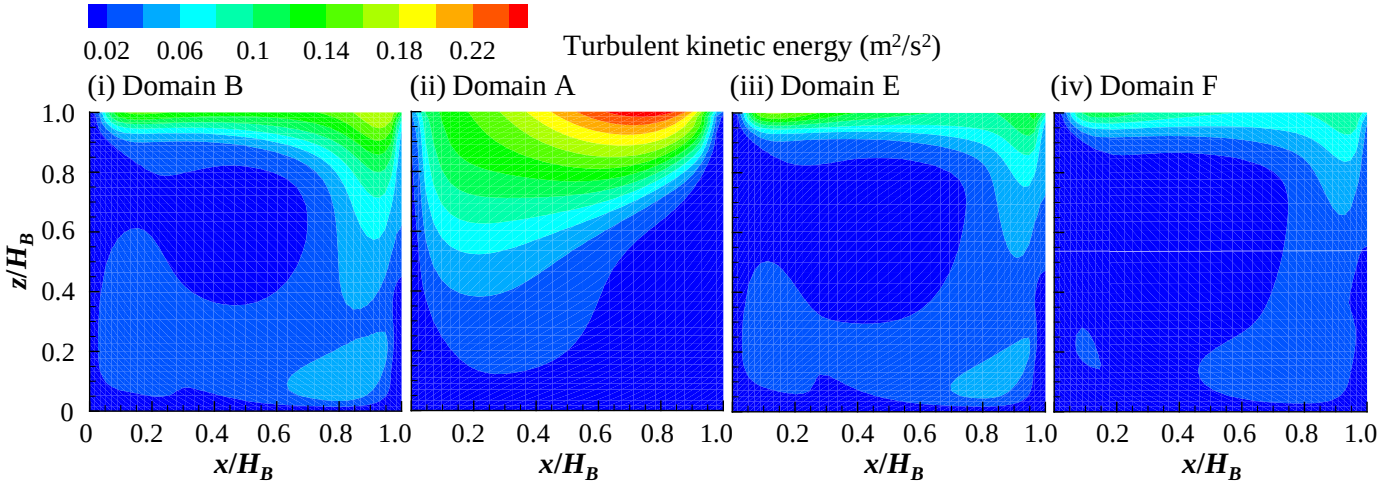

(b) turbulent kinetic energy contour

Figure 7 Evaluation of domain configurations: (a) velocity contour and (b) turbulent kinetic energy contour on the vertical centerplane ($y = 0$) of the street canyon model when using different street canyon configurations, where (i) represents the target street canyon as described in Section 2.

Figure 7 (a) presents the predicted velocity contours on the vertical centerplane of the street canyon using the four computational domains. For Domain A, owing to the effect of the flow impingement in front of the upstream building and the wake flow behind the downstream building, the flow field inside the street canyon is significantly changed when compared to that inside a street canyon with both upstream and downstream buildings (Domain B, the base case). When lifting up the upstream and downstream domain spaces to form a T-shape domain (Domain E), the flow field inside the street canyon is very close to that in Domain B. The flow field predicted using Domain F is still reasonably acceptable, although the flow movements are slightly weaker than those in Domain B. Similar observations can be made based on the comparison of turbulent kinetic energy contours (see Figure 7 (b)) and the comparison of velocity components (Figure 8). Considering also the less computational power needed by Domain E, the evaluations in this section would suggest that it is reliable and accurate to use the Domain E (T-shape domain) to predict the flow field in a street canyon in urban areas.

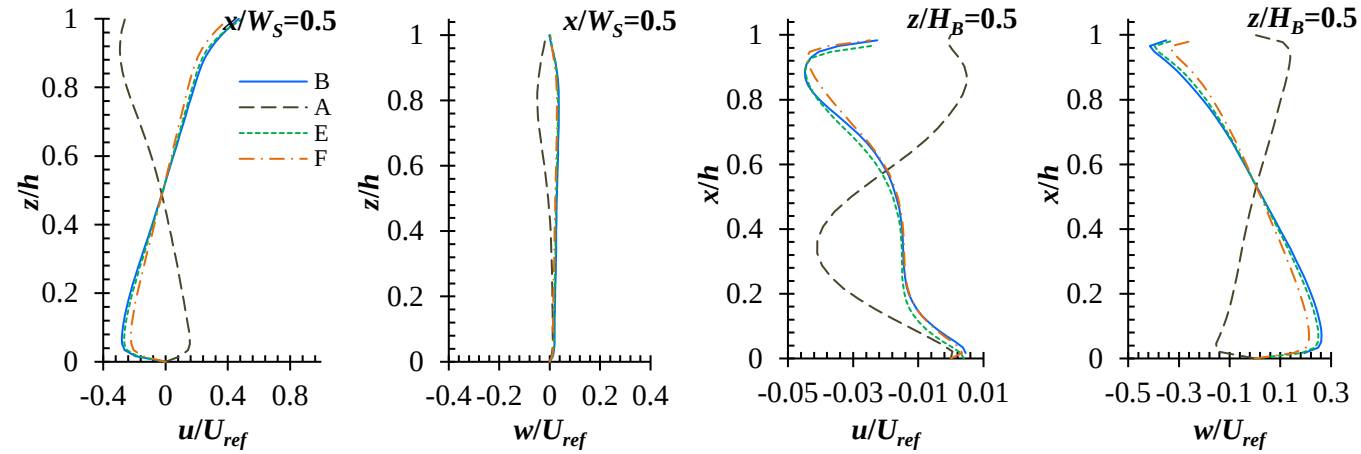

Figure 8 Evaluation of domain configurations: velocity components along the vertical line $x/W_S = 0.5$ and horizontal line $z/H_B = 0.5$ on the centerplane of the target street canyon, where B, A, E and F denote Domain B, Domain A, Domain E and Domain F, respectively.

3.2 Evaluation of dimensions of Domain E

Based on the T-shape computational domain (Domain E in Figure 6 (b)), the influence of domain dimensions, namely upstream length, downstream length and domain height, is examined. When examining the influence of one dimension, e.g. upstream length, other two dimensions, i.e. downstream length and height, remain the same as those in Figure 6 (b). Figure 9 presents the comparison of velocity components (u and w) along the vertical and horizontal centrelines within the street canyon. It can be seen that the influence of downstream length (from $15\,H_B$ to $1\,H_B$) and domain height above the street canyon (from $4\,H_B$ to $1\,H_B$) on the flow field in the street canyon is negligible, suggesting $1\,H_B$ can be used for both the downstream length and domain height above the street canyon. The variation of upstream length (from $5\,H_B$ to $1\,H_B$) results in slight changes in the velocity component in vertical direction (i.e. w). Given that a uniform velocity profile is used at the domain inlet, such an influence of the upstream length should be attributed to the different degrees of inhomogeneity between inflow and approaching flow produced by different upstream lengths [42]. The shorter upstream length can limit the change in the shape of inflow along the computational domain. In practice, approaching flow skims over the top of an upstream building before it reaches a street canyon. Therefore, the upstream ground of the computational domain could be considered as the top of the upstream building, which should be closer to $1\,H_B$ than a longer length. Overall, it is suggested that $1\,H_B$ is an appropriate upstream length.

Note that these appropriate domain dimensions, namely $1\,H_B$ for upstream length, downstream length and height above street canyon, for the T-shape domain (Domain E as shown in Figure 6) resulted from the sensitivity tests conducted in this section are very different from those used for common urban flow simulations using Domain C and Domain D as shown in Figure 1 [34, 35]. The essential reason for this difference in domain dimensions is the different domain configurations used and thus different flow fields around buildings occurred in the two scenarios. The finding on the domain dimensions is very important for saving numerical resources without compromising numerical accuracy.

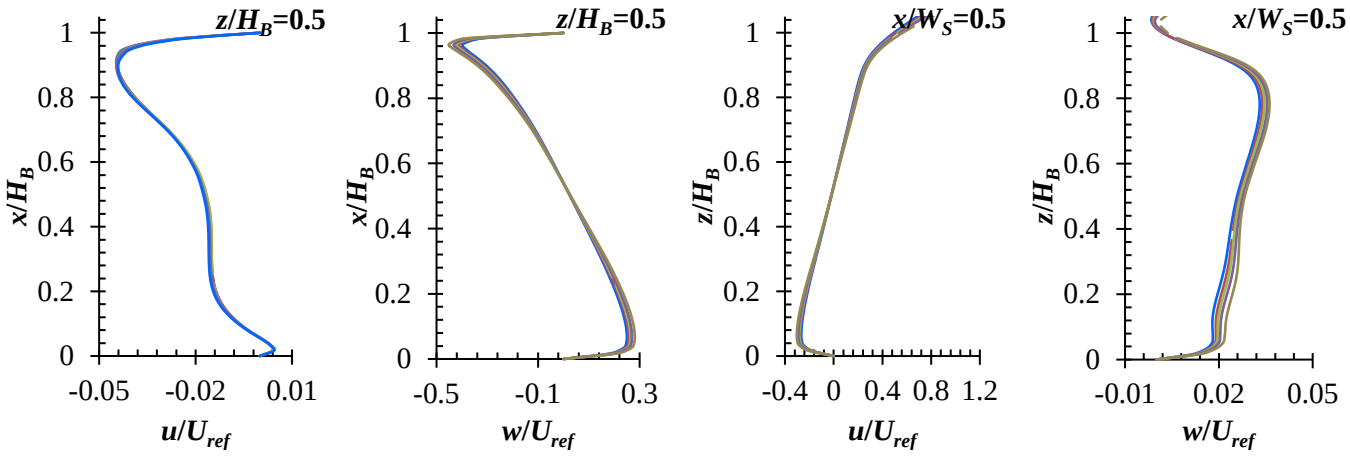

(a) influence of upstream length: from $5\,H_B$, $4\,H_B$, $3\,H_B$, $2\,H_B$ to $1\,H_B$

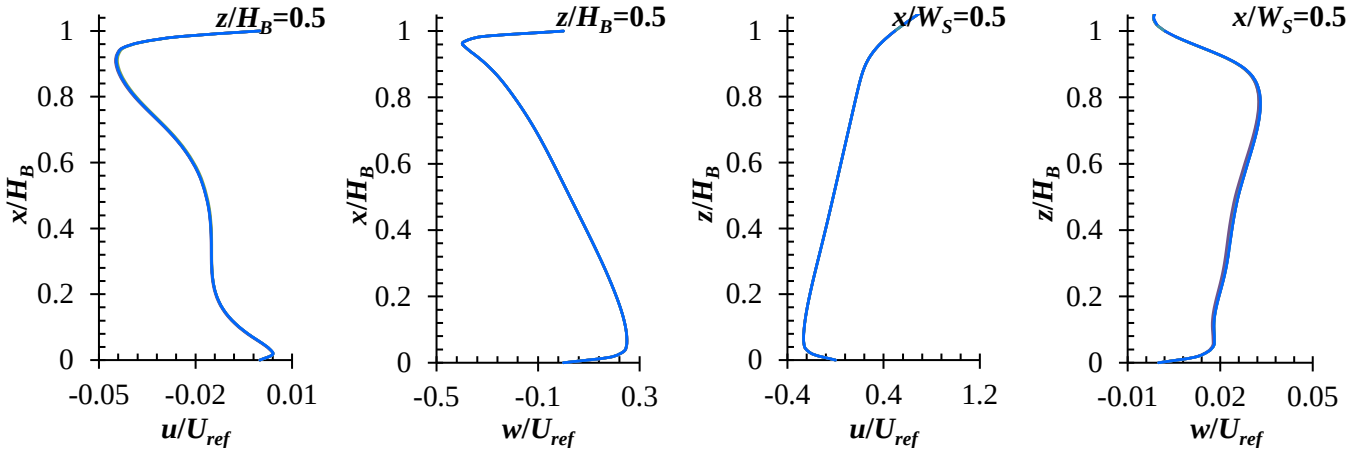

(b) influence of downstream length: from $15\,H_B$, $10\,H_B$, $7\,H_B$, $4\,H_B$, $2\,H_B$ to $1\,H_B$

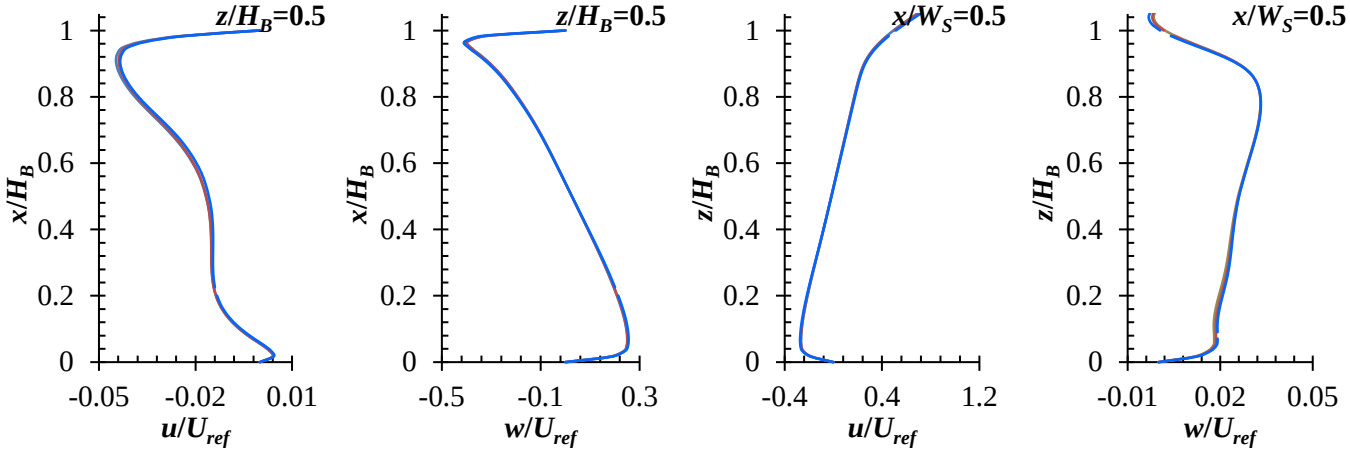

(c) influence of domain height above the street canyon: from $4\,H_B$, $2\,H_B$ to $1\,H_B$

Figure 9 Evaluation of dimensions of Domain E: velocity components along the vertical line x/W_S = 0.5 and horizontal line z/H_B = 0.5 on the centerplane of the street canyon.

3.3 Evaluation of inflow boundary conditions

Based on the domain configuration and domain dimensions resulted from the Sections 3.1 and 3.2, namely the T-shape domain with the upstream length, downstream length and domain height above building equal to $1\,H_B$, this section evaluates the influence of inflow boundary conditions. In addition to the uniform inflow boundary conditions (as used in previous sections), a set of logarithmic law inflow boundary conditions (described by Equations (1)-(3)) was employed and the predicted flow fields by these two compared. This additional set of inflow boundary conditions represents the typical atmospheric boundary layer in urban environment [38- 42]. The reference velocity (U_{ref}) at the height of z_{ref} = 0.1 m (building height) are U_{ref} = 1.8 m/s and the von Karman constant κ is equal to 0.4187. The aerodynamic roughness height (z_0) at the ground is set as 0.00075 m, which is similar with that in a standard atmospheric boundary layer wind tunnel [74]. Based on the values of κ, z_0, U_{ref} and z_{ref}, the friction velocity of atmospheric flow above the ground (u^*) can be determined from Equation (1), which is 0.15 m/s. The turbulent kinetic energy k is fitted with the wind tunnel experiments by Leitl and Schatzmann [74]. Eventually, the model coefficients in Equations (2) and (3) are M_1 = 0.025 and M_2 = 0.41. The empirical constant C_μ is defined empirically as 0.09. Figure 10 presents the nondimensional U, k and ε of the two types of boundary conditions at the domain inlet,

where the U_{av} is the average velocity value on the domain inlet. It must be noted that, for the logarithmic law inflow boundary conditions, the actual inflow profiles are only the parts above the buildings, with z/H_B > 1.0. Such settings were used in previous studies [55, 60], which are also the conditions occurred in practice. The boundary conditions for domain outlet, domain lateral sides, domain top and building surfaces as well as the solver settings are identical to those used in previous sections.

$$U = \frac{u^*}{\kappa}\ln\left(\frac{z+z_0}{z_0}\right) \tag{1}$$

$$k = \sqrt{M_1 \cdot \ln(z+z_0) + M_2} \tag{2}$$

$$\varepsilon = \frac{u^*\sqrt{C_\mu}}{\kappa(z+z_0)}\sqrt{M_1 \cdot \ln(z+z_0) + M_2} \tag{3}$$

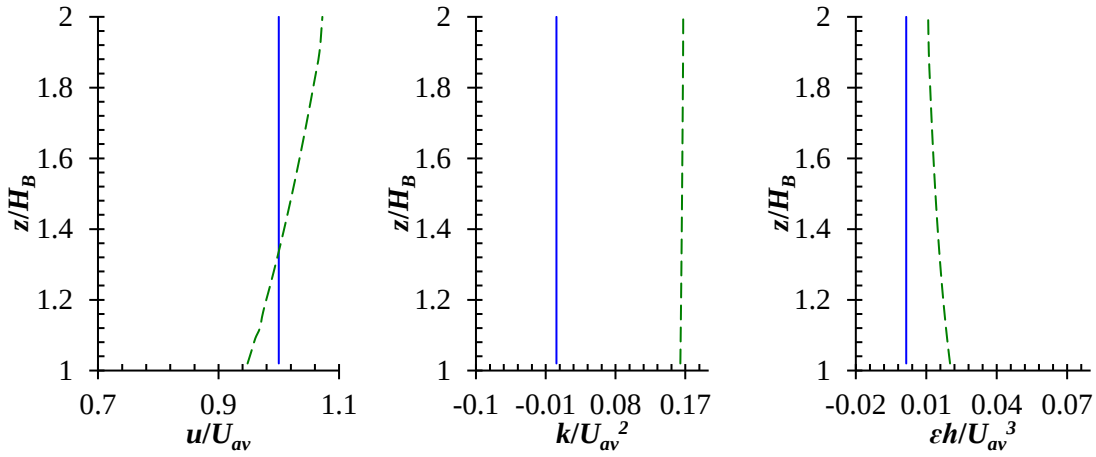

Figure 10 Evaluation of inflow boundary conditions: the two types of inflow boundary conditions, where the blue lines denote the uniform inflow boundary conditions and the dashed green lines the logarithmic law inflow boundary conditions; please note that the values of turbulence kinetic energy (*k*) are all positive.

Figure 11 presents the comparison of velocity components along a vertical and a horizontal line on the centerplane of the street canyon. The basic shape of the two lines is the same. However, the vortex inside the street canyon predicted using the logarithmic law inflow boundary conditions is stronger than that predicted using the uniform inflow boundary conditions. Figure 12 shows the nondimensional turbulent kinetic energy on the vertical centerplane of the street canyon. Despite of the difference in values (probably due to different turbulent characteristics at inlet), the basic trend of turbulent kinetic energy predicted by the two types of inflow conditions is the same. In fact, the uniform inflow would change its shape along the computational domain before it reaches the top of the street canyon [37, 38, 42]. This phenomenon on one hand occurs on building tops in practice and on the other hand would reduce the difference in the approaching flow between the two types of inflow boundary conditions. In addition, the roughness height at the building tops should be much smaller than that above urban ground, where the buildings themselves are roughness elements. Therefore, even if one would use the logarithmic law boundary conditions to represent the free atmospheric boundary layer above building tops, a very thin boundary layer (namely, with a relatively low roughness height) should be applied. In general, the comparison of the velocity and turbulent kinetic energy fields suggest that it is reasonable and appropriate to use the uniform inflow boundary conditions to predict the flow field inside a street canyon within a T-shape domain.

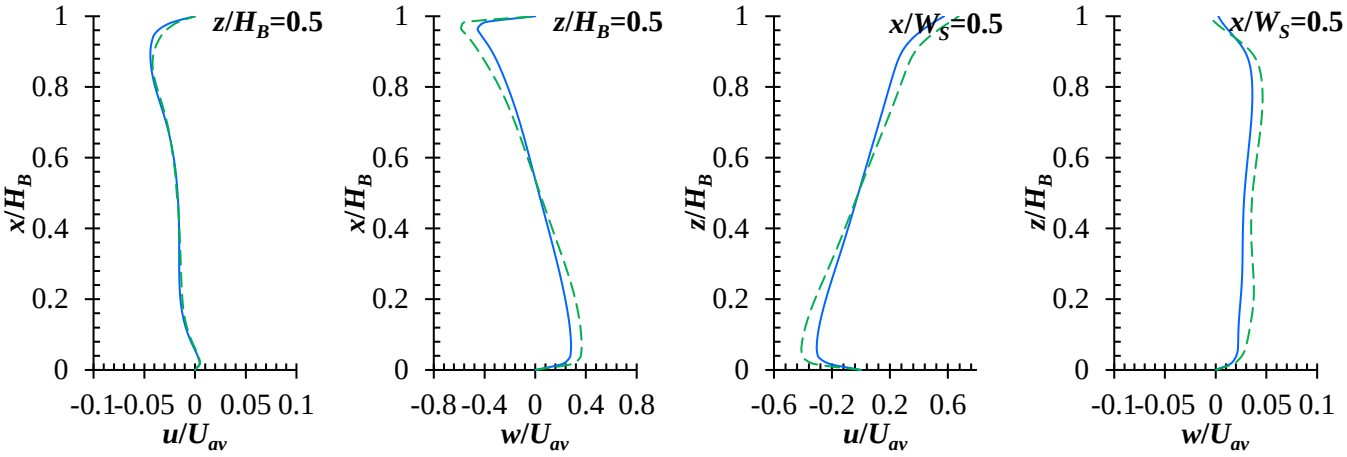

Figure 11 Evaluation of inflow boundary conditions: velocity components along the vertical line $x/W_S = 0.5$ and horizontal line $z/H_B = 0.5$ on the centerplane of the street canyon, where the blue lines denote the use of the uniform inflow boundary conditions and the dashed green lines the logarithmic law inflow boundary conditions.

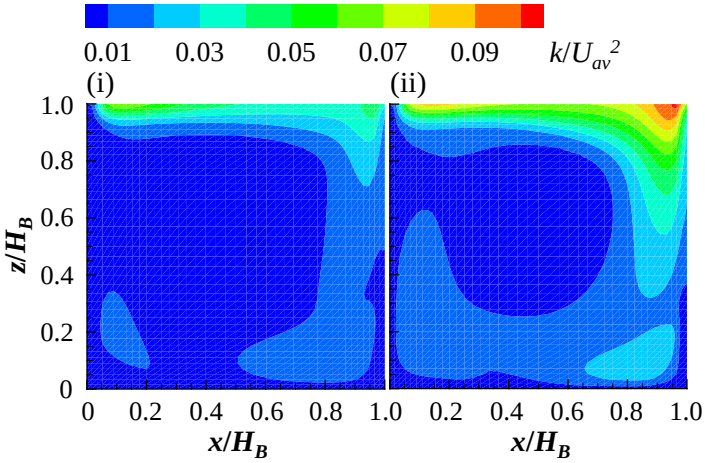

Figure 12 Evaluation of inflow boundary conditions: turbulent kinetic energy on the vertical centerplane of the street canyon; (i) indicates the use of the uniform inflow boundary conditions and (ii) the logarithmic law inflow boundary conditions.

4. Street canyons of AR equal to 0.5 and 2.0

Considering AR equal to 0.5 and 2.0, this section evaluates the influence of domain configuration and domain dimensions on the predicted flow field inside a street canyon, which is intended to verify the validity of the findings obtained based on the case with AR equal to 1.0 (as presented in Section 3). The street configurations for AR equal to 0.5 and 2.0 are described in Section 2.1. The number of building model forming these two street canyons is six and ten, respectively. Therefore, for AR equal to 0.5 and 2.0, the target street canyons are the street canyons between buildings 3 and 4 and between buildings 5 and 6, respectively. The basic computational settings and parameters used for the simulation of these two street canyons are generally the same with those described in Section 2.2, except that the number of cells for the base cases (Domain B) of these two street canyons is 3,264,000 and 2,880,000, respectively.

Figure 13 presents velocity contours for AR = 0.5 predicted using Domain B and Domain E. It shows that the prediction of flow field inside a street canyon using Domain E is acceptably accurate, although the use of the large domain results in a slightly weaker flow vortex and the small domain a slightly stronger flow vortex. As explained in Section 3.2, the difference in flow movement inside the street canyon given by the two versions of Domain E can be attributed to the different approaching

flow profiles they have at the top of the street canyon. Owing to the roughness effect of the domain ground, the lower part of the inflow would decelerate along the upstream of the domain [37, 38, 42]. Therefore, a longer upstream length (large Domain E) would result in a lower wind speed at the lower part of the approaching flow, which certainly leads to a weaker vortex inside the street canyon.

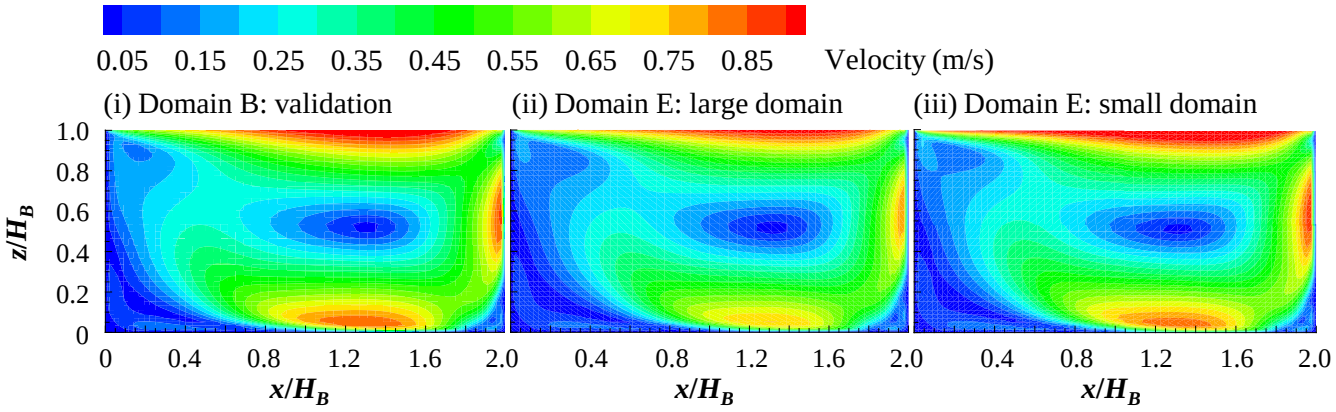

Figure 13 Velocity contours on the vertical centerplane ($y = 0$) of the street canyon with AR = 0.5 predicted using Domain B and Domain E, where the large domain refers to the domain with $5\,H_B$ upstream, $15\,H_B$ downstream and $4\,H_B$ above the street canyon (similar with that in Figure 6 (b)) and the small domain refers to the domain with $1\,H_B$ upstream, downstream and above the street canyon (resulted from Section 3.2).

Figure 14 compares the velocity components in x and z directions inside the target street canyon. In general, simulated velocity components have the same trends with the experimental data. The simulated u values show some discrepancies from the experimental data, while good agreements between simulated and experimental results are found in w values. The experimenters [16] also reported such levels of discrepancies between simulated results and experimental data. Comparison of the velocity components predicted by using the three domains indicates that the use of the small Domain E predicts a very close velocity field inside the street canyon ($z/H_B < 1.0$) to that predicted using the Domain B. At the building top level or above the street canyon ($z/H_B \geq 1.0$), the use of the small Domain E would overpredict the velocity component u. Such an overprediction should be attributed to the larger wind speed occurred at the lower part of the approaching flow (see analysis made for Figure 13). This phenomenon may suggest that the small Domain E is appropriate only if the interest is the flow field inside a street canyon.

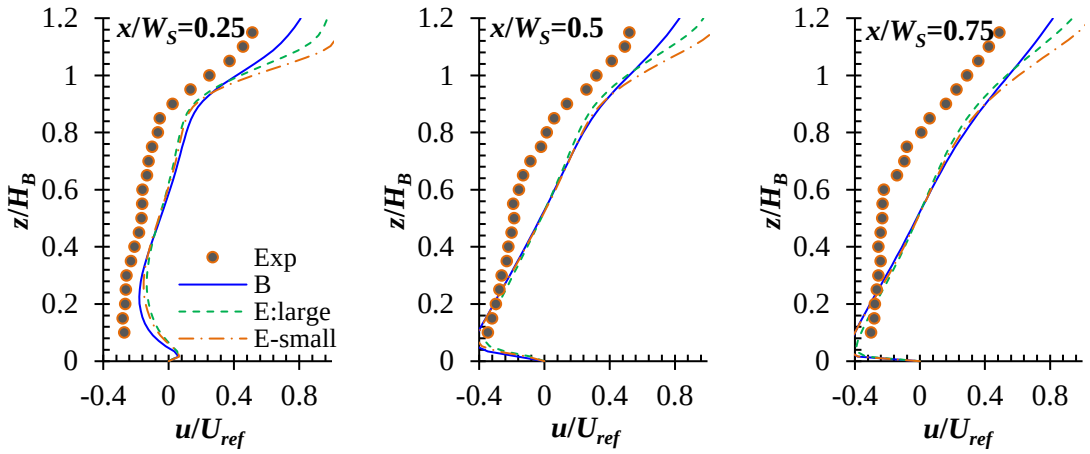

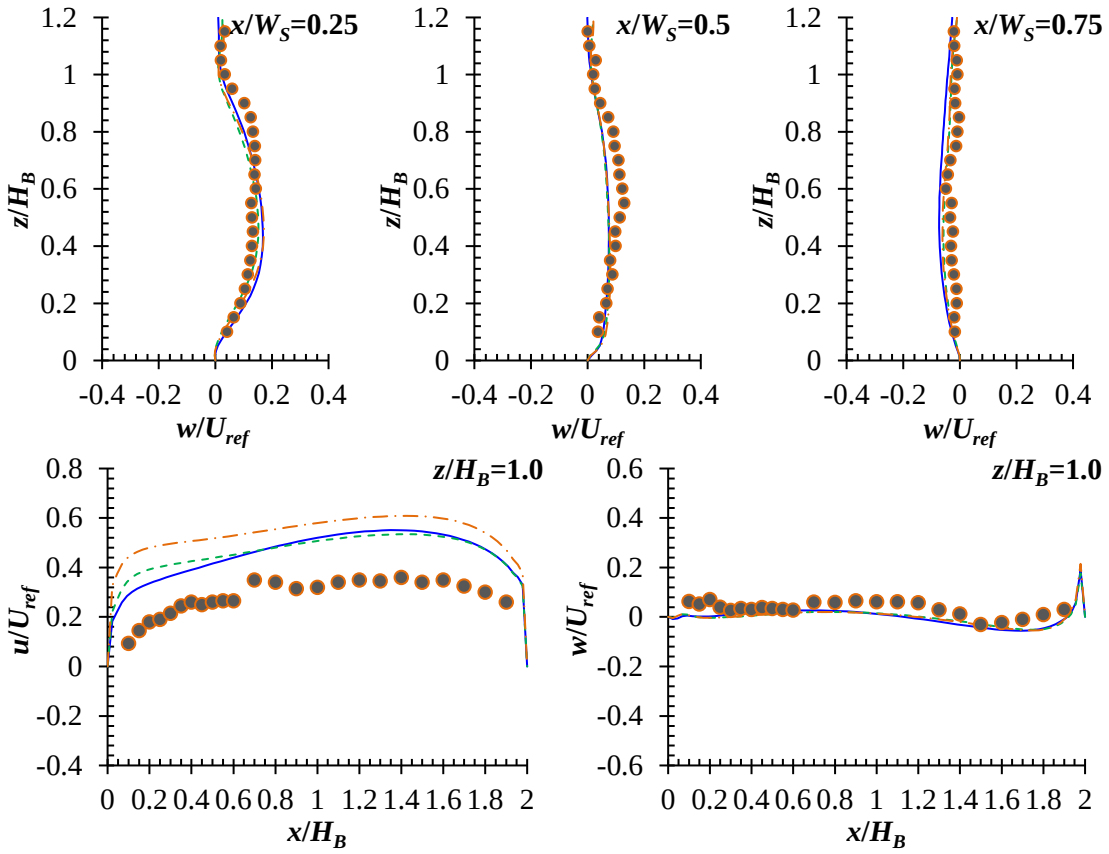

Figure 14 Validation and domain evaluation for AR = 0.5: velocity components in x and z directions along three vertical and two horizontal lines on the vertical centerplane of the target street canyon.

Similar findings are obtained when AR = 2.0 (see Figures 15 and 16). However, the difference in flow movement inside the street canyon predicted by using the large and small Domain E is demonstrated more obviously in the case with AR = 2.0 than those observed in the cases with AR = 0.5 and 1.0. The shape change of the inflow along the computational domain is certainly an important reason. In addition, previous studies (e.g., as reviewed by Ai and Mak [2]) indicate that the flow movement inside a street canyon is strongly dependent on the establishment of the coupling between the street canyon and its above atmosphere, which is further determined by both the wind speed above the street canyon and the aspect ratio of the street canyon. This is especially the case for a relatively deep street canyon. However, exploring the relationship between the flow field inside and outside the street canyon is out of the focus of this study. In general, results presented in this section (Figures 13-16) tend to suggest that the small Domain E is an appropriate choice for predicting flow field inside a street canyon of AR = 0.5 and 2.0, when considering both the computational cost and the capability of revealing basic flow characteristics inside a street canyon in urban areas.

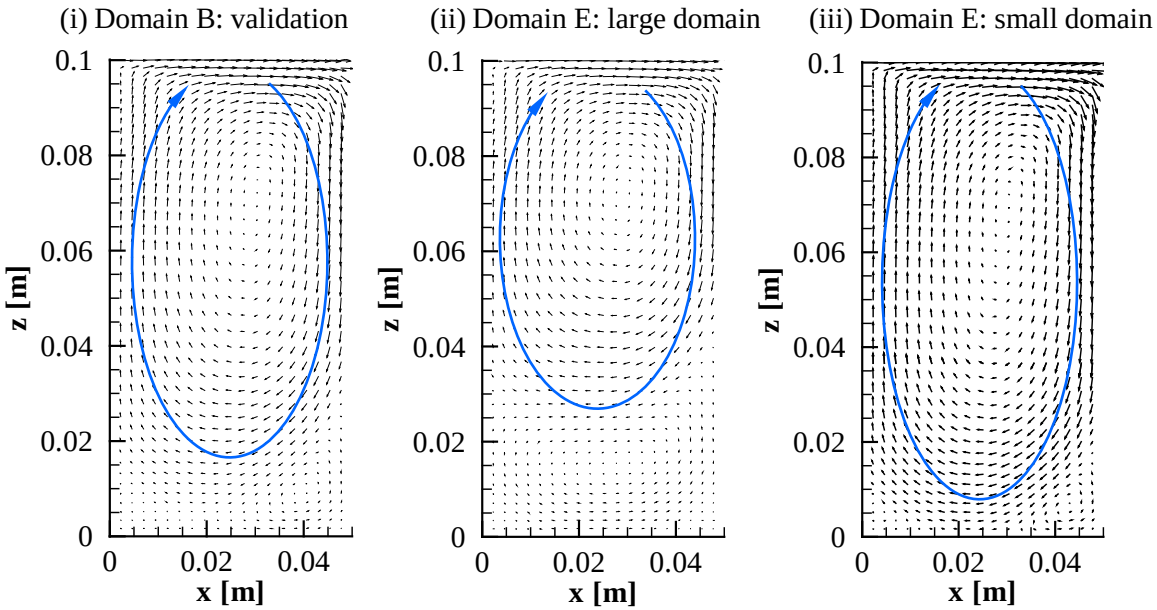

Figure 15 Velocity vectors on the vertical centerplane ($y = 0$) within the street canyon of AR = 2.0 predicted using Domain B and Domain E, where the large domain refers to the domain with $5\,H_B$ upstream, $15\,H_B$ downstream and $4\,H_B$ above the street canyon (similar with that in Figure 6 (b)) and the small domain refers to the domain with $1\,H_B$ upstream, downstream and above the street canyon (resulted from Section 3.2).

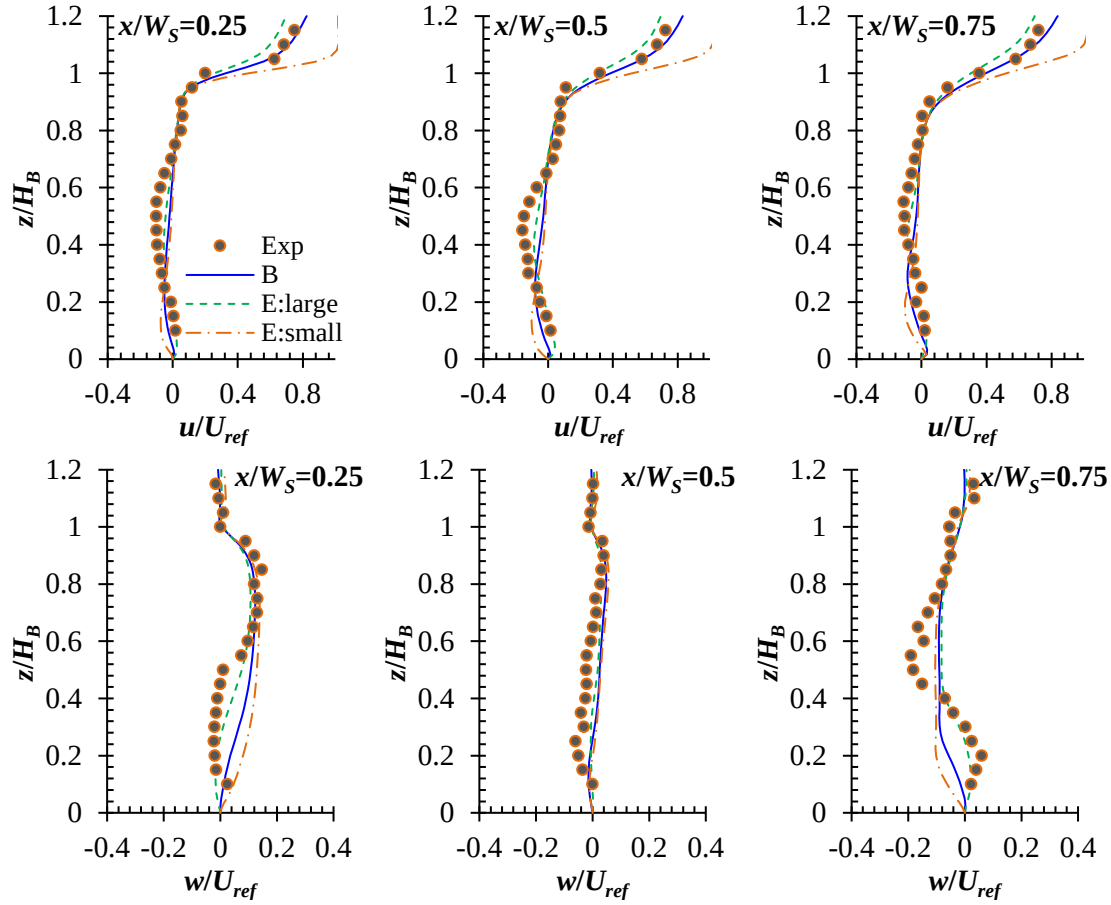

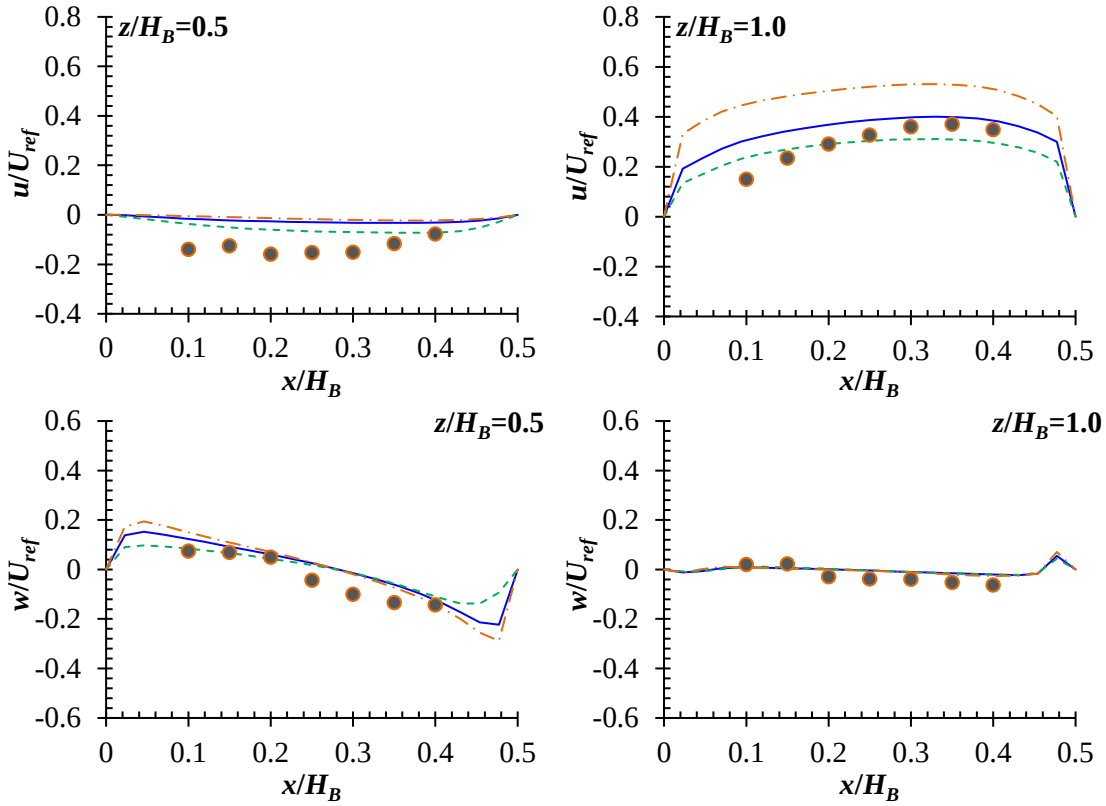

Figure 16 Validation and domain evaluation for AR = 2.0: velocity components in x and z directions along three vertical and two horizontal lines on the vertical centerplane of the target street canyon.

5. Discussion

This study focuses on examining three important computational parameters that could influence the accuracy of CFD simulation of flow field inside a street canyon in urban areas and the computational cost. The three parameters are configuration of computational domain, dimensions of computational domain and inflow boundary conditions. It presumes that other computational parameters, such as computational grid, boundary conditions (except on inlet), solution methods and convergence criteria, should follow the recommendations of the existing general best practice guidelines for CFD simulation of urban aerodynamics.

This study considers only the perpendicularly incident wind direction, because of two main reasons. First, most wind/water tunnel experiments and CFD simulations as reviewed in the paper investigate only the cases under perpendicularly incident wind, as they represent the worst wind field inside a street canyon for pollutant dilution. Second, the experimental data is available only for the cases under perpendicularly incident wind. Despite of these reasons, it is still worthwhile to examine the validity of the findings arisen from the perpendicular wind direction to oblique and parallel wind directions.

Only flow field is examined in this study. Although the accurate prediction of flow field in a street canyon is the basic prerequisite of accurate prediction of other atmospheric processes in a street canyon, further investigations are needed to examine the validity of the findings for flow field to other atmospheric processes, such as pollutant dispersion and ventilation of nearby buildings.

Only the RANS model, specifically RNG $k-\varepsilon$ model, is used. It is known that the RANS models provide effective time-averaged flow solutions, which, however, largely cancel out the contributions of temporal fluctuations. In contrast, the large eddy simulation (LES) model can capture the flow intermittencies and separations around the street canyon more accurately and thus can provide more realistic results. The validity of the findings to the LES model requires further examinations.

6. Conclusions

Considering three AR values (0.5, 1.0 and 2.0), this study evaluates three computational settings – domain configuration, domain dimensions and inflow boundary conditions – that are important to CFD simulation of atmospheric flow in a long street canyon in an urban context. This study allows the following conclusions to be drawn:

- Flow field inside a long street canyon in an urban context can be well predicted using a T-shape computational domain (Domain E in this study), which, however, cannot be reasonably predicted using a conventional domain with an isolated street canyon exposing in an atmospheric boundary layer (Domain A in this study).
- It is appropriate to use a small T-shape domain, namely with 1 H_B for upstream length, downstream length and height above a long street canyon to predict the flow field inside the street canyon.
- For the simplified T-shape computational domain, it is reasonable to use the uniform inflow boundary conditions to predict the flow field inside a long street canyon, as it closely represents the free atmospheric boundary layer above street canyons in urban environments.

Acknowledgement

The work described in this paper was financially supported by a grant from the Environment and Conservation Fund of Hong Kong (Project ECF 18/2014).

References

[1] T.R. Oke, Boundary Layer Climates, second ed., Routledge, New York, 1987.
[2] Z.T. Ai, C.M. Mak, From street canyon microclimate to indoor environmental quality in naturally ventilated urban buildings: issues and possibilities for improvement, Build. Environ. 94 (2015) 489-503.
[3] C. Georgakis, M. Santamouris, Experimental investigation of air flow and temperature distribution in deep urban canyons for natural ventilation purposes, Energ. Buildings 38 (2006) 367-376.
[4] E. Andreou, K. Axarli, Investigation of urban canyon microclimate in traditional and contemporary environment: Experimental investigation and parametric analysis, Renew. Energ. 43 (2012) 354-363.
[5] Y. Nakamura, T.R. Oke, Wind, temperature and stability conditions in an east-west oriented urban canyon, Atmos. Environ. 22(12) (1988) 2691-2700.
[6] I. Eliasson, B. Offerle, C.S.B. Grimmond, S. Lindqvist, Wind fields and turbulence statistics in an urban street canyon, Atmos. Environ. 40 (2006) 1-16.
[7] M. Santamouris, N. Papanikolaou, I. Koronakis, I. Livada, D. Asimakopoulos, Thermal and air flow characteristics in a deep pedestrian canyon under hot weather conditions, Atmos. Environ. 33 (1999) 4503-4521.
[8] A.J. Manning, K.J. Nicholson, D.R. Middleton, S.C. Rafferty, Field study of wind and traffic to test a street canyon pollution model, Environ. Monit. Assess. 60 (2000) 283-313.
[9] K. Niachou, I. Livada, M. Santamouris, Experimental study of temperature and airflow distribution inside an urban street canyon during hot summer weather conditions – Part 2: Airflow analysis, Build. Environ. 43 (2008) 1393-1403.
[10] H. Boogaard, N.A.H. Janssen, P.H. Fischer, G.P.A. Kos, E.P. Weijers, F.R. Cassee, et al., Contrasts in oxidative potential and other particulate matter characteristics collected near major streets and background locations, Environ. Health Perspect. 120(2) (2012) 185-191.
[11] L. Zhao, X. Wang, Q. He, H. Wang, G. Sheng, L. Chan, et al., Exposure to hazardous volatile organic compounds, PM_{10} and CO while walking along streets in urban Guangzhou, China, Atmos. Environ. 38 (2004) 6177-6184.
[12] Y. Cheng, S.C. Lee, Y. Gao, L. Cui, W. Deng, J. Cao, et al., Real-time measurements of $PM_{2.5}$, $PM_{10\text{-}2.5}$, and BC in an urban street canyon, Particuology 20 (2015) 134-140.
[13] T. Nielsen, Traffic contribution of polycyclic aromatic hydrocarbons in the center of a large city, Atmos. Environ. 20 (1996) 3481-3490.
[14] J.J. Baik, R.S. Park, H.Y. Chun, J.J. Kim, A laboratory model of urban street-canyon flows, J. Appl. Meteor. 39 (2000) 1592-1600.

[15] M. Pavageau, M. Schatzmann, Wind tunnel measurements of concentration fluctuations in an urban street canyon, Atmos. Environ. 33 (1999) 3961-3971.
[16] X.X. Li, D.Y.C. Leung, C.H. Liu, Physical modelling of flow field inside urban street canyons, J. Appl. Meteorol. Clim. 47 (2008) 2058-2067.
[17] P. Salizzoni, L. Soulhac, P. Mejean, Street canyon ventilation and atmospheric turbulence, Atmos. Environ. 43 (2009) 5056-5067.
[18] R. Kellnerova, L. Kukacka, K. Jurcakova, V. Uruba, Z. Janour, PIV measurement of turbulent flow within a street canyon: Detection of coherent motion, J. Wind Eng. Ind. Aerod. 104-106 (2012) 302-313.
[19] P. Kastner-Klein, E. Fedorovich, M.W. Rotach, A wind tunnel study of organised and turbulent air motions in urban street canyons, J. Wind Eng. Ind. Aerod. 89 (2001) 849-861.
[20] C. Gromke, R. Buccolieri, S. Di Sabatino, B. Ruck, Dispersion study in a street canyon with tree planting by means of wind tunnel and numerical investigations – Evaluation of CFD data with experimental data, Atmos. Environ. 42 (2008) 8640-8650.
[21] L. Stabile, F. Arpino, G. Buonanno, A. Russi, A. Frattolillo, A simplified benchmark of ultrafine particle dispersion in idealized urban street canyons: A wind tunnel study, Build. Environ. 93 (2015) 186-198.
[22] J. Allegrini, V. Dorer, J. Carmeliet, Wind tunnel measurements of buoyant flows in street canyons, Build. Environ. 59 (2013) 315-326.
[23] W.H. Snyder, Guideline for fluid modelling of atmospheric diffusion, meteorology and assessment. Research Triangle Park, NC, Division Environmental Sciences Research Laboratory, U.S. Environmental Protection Agency, 1981.
[24] R.N. Meroney, Wind tunnel and numerical simulation of pollution dispersion: A hybrid approach. Invited Lecture, Croucher Advanced Study Institute, Hong Kong University of Science and Technology, 6-10 December, 2004.
[25] B. Blocken, 50 years of computational wind engineering: Past, present and future, J. Wind Eng. Ind. Aerod. 129 (2014) 69-102.
[26] J.J. Kim, J.J. Baik, Urban street-canyon flows with bottom heating, Atmos. Environ. 35 (2001) 3395-3404.
[27] C.H. Liu, M.C. Barth, D.Y.C. Leung, Large-eddy simulation of flow and pollutant transport in street canyons of different building-height-to-street-width ratios, J. Appl. Meteor. 43 (2004) 1410-1424.
[28] X. Xie, Z. Huang, J. Wang, The impact of urban street layout on local atmospheric environment, Build. Environ. 41 (2006) 1352-1363.
[29] P. Moonen, V. Dorer, J. Carmeliet, Evaluation of the ventilation potential of courtyards and urban street canyons using RANS and LES, J. Wind Eng. Ind. Aerod. 99 (2011) 414-423.
[30] K.H. Kwak, J.J. Baik, K.Y. Lee, Dispersion and photochemical evolution of reactive pollutants in street canyons, Atmos. Environ. 70 (2013) 98-107.
[31] J. Allegrini, V. Dorer, J. Carmeliet, Buoyant flows in street canyons: Validation of CFD simulations with wind tunnel measurements, Build. Environ. 72 (2014) 63-74.
[32] J. Hang, M. Lin, D.C. Wong, X. Wang, B. Wang, R. Buccolieri, On the influence of viaduct and ground heating on pollutant dispersion in 2D street canyons and toward single-sided ventilated buildings, Atmos. Pollut. Res. 7(5) (2016) 817-832.
[33] M. Casey, T. Wintergerste, Best Practice Guidelines, ERCOFTAC Special Interest Group on Quality and Trust in Industrial CFD, ERCOFTAC, Brussels, 2000.
[34] J. Franke, A. Hellsten, H. Schlunzen, B. Carissimo, Best practice guideline for the CFD simulation of flows in the urban environment – COST Action 732. COST office, 2007.
[35] Y. Tominaga, A. Mochida, R. Yoshie, H. Kataoka, T. Nozu, M. Yoshikawa, T. Shirawasa, AIJ guidelines for practical applications of CFD to pedestrian wind environment around buildings, J. Wind Eng. Ind. Aerod. 96(10-11) (2008) 1749-1761.
[36] B. Blocken, C. Gualtieri, Ten iterative steps for model development and evaluation applied to computational fluid dynamics for environmental fluid mechanics, Environ. Model. Softw. 33 (2012) 1-22.
[37] P.J. Richards, R. Hoxey, Appropriate boundary conditions for computational wind engineering models using the k – ε turbulence model, J. Wind Eng. Ind. Aerod. 46-47 (1993) 145-153.

[38] B. Blocken, T. Stathopoulos, J. Carmeliet, CFD simulation of the atmospheric boundary layer: wall function problems, Atmos. Environ. 41 (2007) 238-252.
[39] D. Hargreaves, N. Wright, On the use of the k − ε model in commercial CFD software to model the neutral atmospheric boundary layer, J. Wind Eng. Ind. Aerod. 95 (2007) 355-369.
[40] C. Gorlé, J. van Beeck, P. Rambaud, G. Van Tendeloo, CFD modeling of small particle dispersion: the influence of the turbulence kinetic energy in the atmospheric boundary layer, Atmos. Environ. 43 (2009) 673-681.
[41] Y. Yang, M. Gu, S. Chen, X. Jin, H. Jin, New inflow boundary conditions for modeling the neutral equilibrium atmospheric boundary layer in computational wind engineering, J. Wind Eng. Ind. Aerod. 97 (2009) 88-95.
[42] Z.T. Ai, C.M. Mak, CFD simulation of flow and dispersion around an isolated building: effect of inhomogeneous ABL and near-wall treatment, Atmos. Environ. 77 (2013) 568-578.
[43] T. van Hooff, B. Blocken, Coupled urban wind flow and indoor natural ventilation modelling on a high-resolution grid: a case study for the Amsterdam ArenA stadium, Environ. Model. Softw. 25(1) (2010) 51-65.
[44] Z.T. Ai, C.M. Mak, Modeling of coupled urban wind flow and indoor air flow on a high-density near-wall mesh: Sensitivity analyses and case study for single-sided ventilation, Environ. Model. Softw. 60 (2014) 57-68.
[45] E.S.P. So, A.T.Y. Chan, A.Y.T. Wong, Large-eddy simulations of wind flow and pollutant dispersion in a street canyon, Atmos. Environ. 39 (2005) 3573-3582.
[46] P. Kastner-Klein, E.J. Plate, Wind-tunnel study of concentration fields in street canyons, Atmos. Environ. 33 (1999) 3973-3979.
[47] K. Nazridoust, G. Ahmadi, Airflow and pollutant transport in street canyons, J. Wind Eng. Ind. Aerod. 94 (2006) 491-522.
[48] P.A. Mirzaei, F. Haghighat, Pollution removal effectiveness of the pedestrian ventilation system, J. Wind Eng. Ind. Aerod. 99 (2011) 46-58.
[49] H. Kikumoto, R. Ooka, A numerical study of air pollutant dispersion with biomolecular chemical reactions in an urban street canyon using large-eddy simulation, Atmos. Environ. 54 (2012) 456-464.
[50] R. Buccolieri, C. Gromke, S. Di Sabatino, B. Ruck, Aerodynamic effects of trees on pollutant concentration in street canyons, Sci. Total Environ. 407 (2009) 5247-5256.
[51] R. Buccolieri, S.M. Salim, L.S. Leo, S. Di Sabatino, A. Chan, P. Ielpo, G. de Gennaro, C. Gromke, Analysis of local scale tree-atmosphere interaction on pollutant concentration in idealized street canyons and application to a real urban junction, Atmos. Environ. 45 (2011) 1702-1713.
[52] E. Solazzo, X. Cai, S. Vardoulakis, Modelling wind flow and vehicle-induced turbulence in urban streets, Atmos. Environ. 42 (2008) 4918-4931.
[53] S.M. Salim, R. Buccolieri, A. Chan, S. Di Sabatino, Numerical simulation of atmospheric pollutant dispersion in an urban street canyon: Comparison between RANS and LES, J. Wind Eng. Ind. Aerod. 99 (2011) 103-113.
[54] P. Moonen, C. Gromke, V. Dorer, Performance assessment of Large Eddy Simulation (LES) for modelling dispersion in an urban street canyon with tree planting, Atmos. Environ. 75 (2013) 66-76.
[55] J.J. Baik, Y.S. Kang, J.J. Kim, Modeling reactive pollutant dispersion in an urban street canyon, Atmos. Environ. 41 (2007) 934-949.
[56] X.X. Li, C.H. Liu, D.Y.C. Leung, Large-eddy simulation of flow and pollutant dispersion in high-aspect-ratio urban street canyons with wall model, Bound.-Layer Meteor. 129 (2008) 249-268.
[57] P. Kumar, A. Garmory, M. Ketzel, R. Berkowicz, R. Britter, Comparative study of measured and modelled number concentrations of nanoparticles in an urban street canyon, Atmos. Environ. 43 (2009) 949-958.
[58] L.H. Hu, R. Huo, D. Yang, Large eddy simulation of fire-induced buoyancy driven plume dispersion in an urban street canyon under perpendicular wind flow, J Hazard. Mater. 166 (2009) 394-406.
[59] Y.W. Zhang, Z.L. Gu, Y. Cheng, S.C. Lee, Effect of real-time boundary wind conditions on the air flow and pollutant dispersion in an urban street canyon – Large eddy simulations, Atmos. Environ. 45 (2011) 3352-3359.

[60] J.J. Baik, K.H. Kwak, S.B. Park, Y.H. Ryu, Effects of building roof greening on air quality in street canyons, Atmos. Environ. 61 (2012) 48-55.
[61] D.M.S. Madalozzo, A.L. Braun, A.M. Awruch, I.B. Morsch, Numerical simulation of pollutant dispersion in street canyons: Geometric and thermal effects, Appl. Math. Model. 38 (2014) 5883-5909.
[62] V.D. Assimakopoulos, H.M. ApSimon, N. Moussiopoulos, A numerical study of atmospheric pollutant dispersion in different two-dimensional street canyon configurations, Atmos. Environ. 37 (2003) 4037-4049.
[63] X. Xie, C.H. Liu, D.Y.C. Leung, Impact of building facades and ground heating on wind flow and pollutant transport in street canyons, Atmos. Environ. 41 (2007) 9030-9049.
[64] W.C. Cheng, C.H. Liu, D.Y.C. Leung, On the correlation of air and pollutant exchange for street canyons in combined wind-buoyancy-driven flow, Atmos. Environ. 43 (2009) 3682-3690.
[65] W.C. Cheng, C.H. Liu, Large-eddy simulation of turbulent transports in urban street canyons in different thermal stabilities, J. Wind Eng. Ind. Aerod. 99 (2011) 434-442.
[66] C.H. Liu, W.C. Cheng, T.C.Y. Leung, D.Y.C. Leung, On the mechanism of air pollutant re-entrainment in two-dimensional idealized street canyons, Atmos. Environ. 45 (2011) 4763-4769.
[67] Y. Takano, P. Moonen, On the influence of roof shape on flow and dispersion in an urban street canyon, J. Wind Eng. Ind. Aerod. 123 (2013) 107-120.
[68] Fluent, ANSYS FLUENT 13.0 Theory Guide. Turbuelnce, Canonsburg, PA, ANSYS Inc., 2010.
[69] V. Yakhot, S.A. Orszag, Renormalization group analysis of turbulence: 1 Basic theory, J. Sci. Comput. 1 (1986) 1-51.
[70] Y. Tominaga, T. Stathopoulos, Numerical simulation of dispersion around an isolated cubic building: comparison of various types of $k-\varepsilon$ models, Atmos. Environ. 43 (2009) 3200-3210.
[71] Z.T. Ai, C.M. Mak, J.L. Niu, Numerical investigation of wind-induced airflow and interunit dispersion characteristics in multistory residential buildings, Indoor Air 23 (2013) 417-429.
[72] Z.T. Ai, C.M. Mak, A study of interunit dispersion around multistory buildings with single-sided ventilation under different wind directions, Atmos. Environ. 88 (2014) 1-13.
[73] M. Wolfshtein, The velocity and temperature distribution of one-dimensional flow with turbulence augmentation and pressure gradient, Int. J. Heat Mass Transf. 12 (1969) 301-318.
[74] B. Leitl, M. Schatzmann, CEDVAL at Hamburg University, 1998, available at: http://www.mi.zmaw.de/index.php?id=433, accessed in June 2016.